H31A-1406

# Effects of Explicit Convection on Global Land-atmosphere Coupling in the Superparameterized CAM

Jian Sun*, and Mike Pritchard
Department of Earth System Science, University of California, Irvine
*contact: jiansun@uci.edu

## Introduction

Current global climate models may be prone to producing land-atmosphere coupling dynamics that are too strong or simplistic. Cumulus and convection parameterizations are natural culprits but the effect of bypassing them with explicitly resolved convection on global land-atmosphere coupling dynamics has not been explored systematically. We apply a suite of modern land-atmosphere coupling diagnostics to isolate the effect of cloud superparameterization (SP) in the Community Atmosphere Model v3.5, focusing on both the land segment (i.e., soil moisture and evapotranspiration relationship) and atmospheric segment (i.e., evapotranspiration and precipitation relationship) in the water pathway of the land-atmosphere feedback loop. The land-atmosphere mechanisms are further diagnosed with the mixing diagram approach at process levels. The ARM Best Estimate (ARMBE) data products are used as benchmark values for model validation in the Southern Great Plains (SGP).

## Land-atmosphere interactions

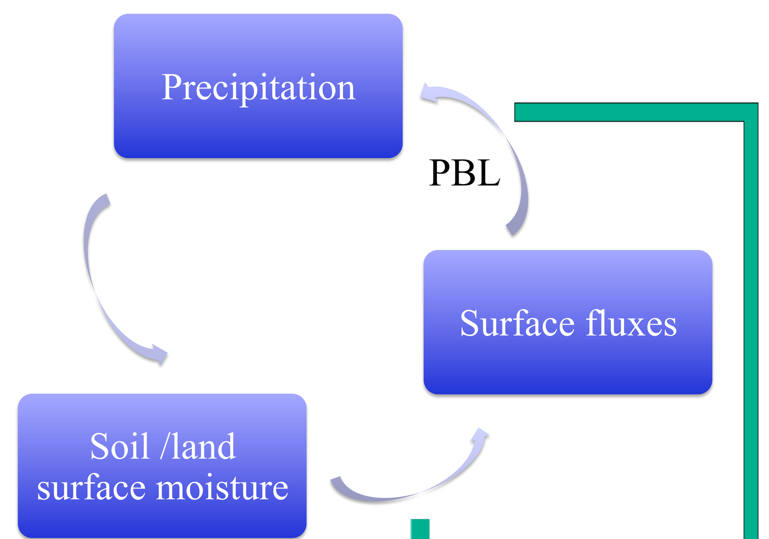


Processes involved in the soil moisture – precipitation coupling and feedback loop:

- Soil moisture plays a big role in surface flux partitioning. Wetter soil supplies more water for evapotranspiration.
- Both sensible and latent heat fluxes affect the planetary boundary layer (PBL) growth and further rainfall triggering, but the mechanisms are complex and the effects are most uncertain in the feedback loop.
- Precipitation generally increases soil moisture.

## Superparameterized CAM

The superparameterized version of CAM has a CRM embedded in each GCM grid:

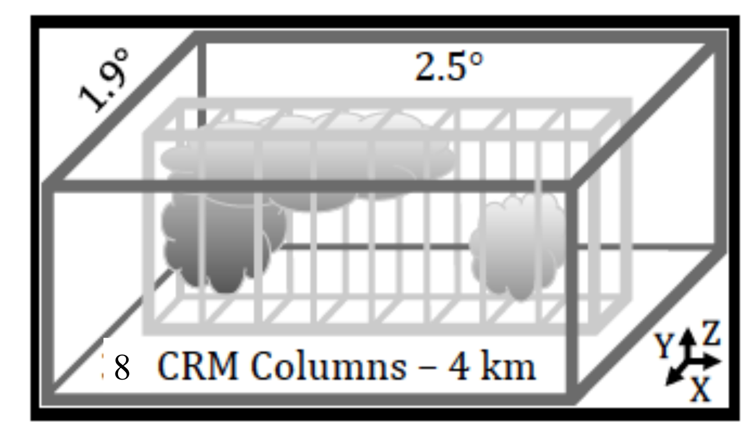


Model set-up and simulations:

- Two models (semi-Lagrangian CAM3.5 and SPCAM3.5) run with same ocean climatology;
- 20-year simulations with first 5-years disregarded as spin-up;
- T42 (~2.8°) exterior spatial resolution; 4km CRM resolution and 128-km CRM extent;
- Daily and hourly output used for coupling indices calculations.

## Terrestrial segment

Terrestrial coupling index (Dirmeyer 2011) accounting for soil moisture and surface fluxes coupling strength:

$$I_\phi = s_w \beta_\phi$$

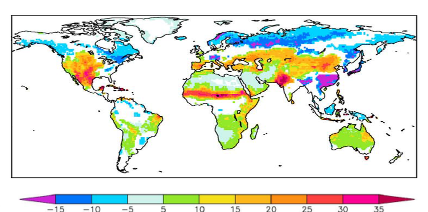

Figure 1: $I_{LH}$ of GSWP-2 data (10 JJAs), figure from Dirmeyer (2011).

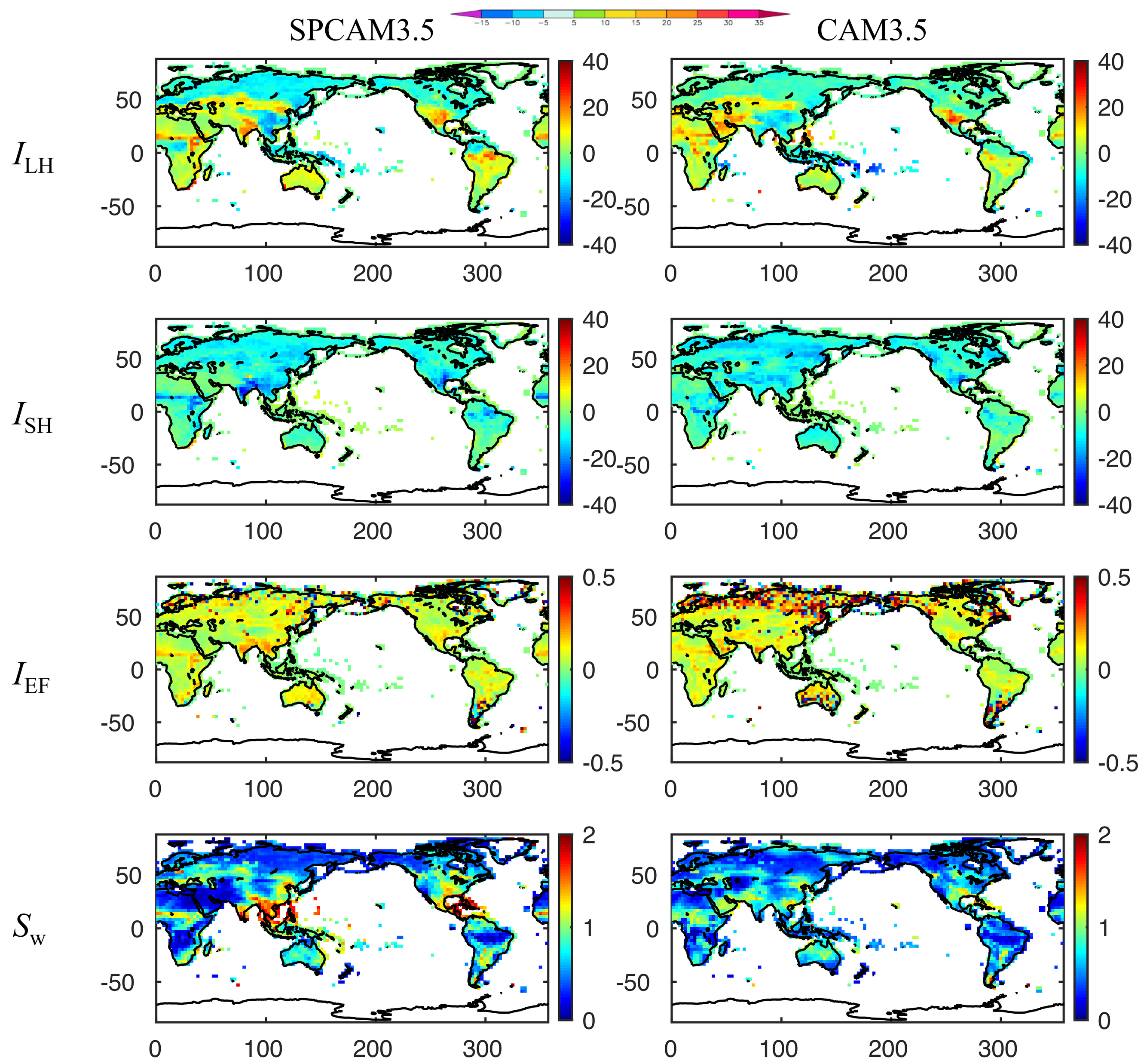


Figure 2: (First 3 rows) JJA terrestrial coupling indices of soil moisture (top 3 cm) versus latent heat flux (LH), sensible heat flux (SH) and evaporation fraction (EF). (Bottom row) standard deviation of soil moisture (SM).

- Regional patterns of the terrestrial coupling indices are different between the models, although the overall magnitudes of the coupling strength are similar.
- The model discrepancies occur in different regions for different fluxes in the coupling index. SPCAM3.5 reduces the coupling strength of (LH, SM) in central North America, Middle East, North Africa, while strengthens the coupling signal in India. As for the coupling index of (SH,SM), SPCAM3.5 basically increases the coupling strength in Indo-China, India and Central Africa. Calculating the coupling index with EF, the models are harder to distinguish, although SPCAM3.5 increases the coupling signal in Indo-China and India, while reduces the coupling signal in Middle East.
- The regions displaying different strength of the terrestrial coupling signals generally show different variations of soil moisture (resulted from precipitation).

## Atmospheric segment

Triggering feedback strength (TFS) and amplification feedback strength (AFS) indices (Findell et al. 2011) accounting for surface fluxes and precipitation coupling strength:

$$\mathrm{TFS} = \sigma_{\mathrm{EF}} \frac{\partial \Gamma(r)}{\partial \mathrm{EF}} \qquad \mathrm{AFS} = \sigma_{\mathrm{EF}} \frac{\partial \mathrm{E}[r]}{\partial \mathrm{EF}}$$

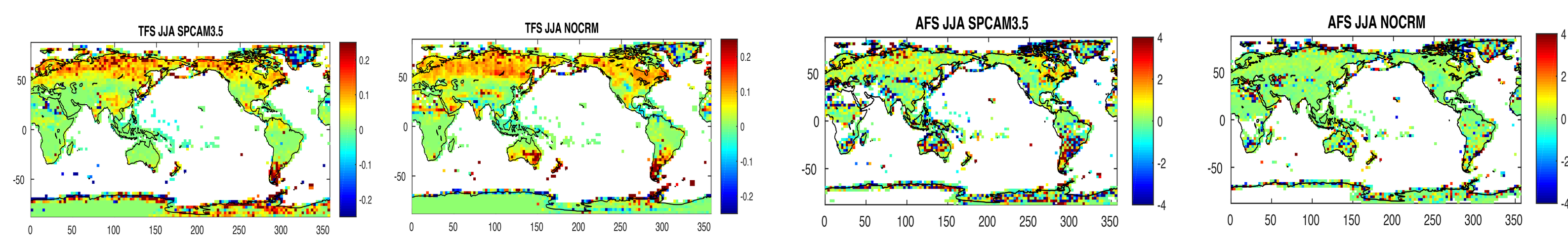


Figure 3: Global distribution of TFS and AFS indices in 15 JJAs

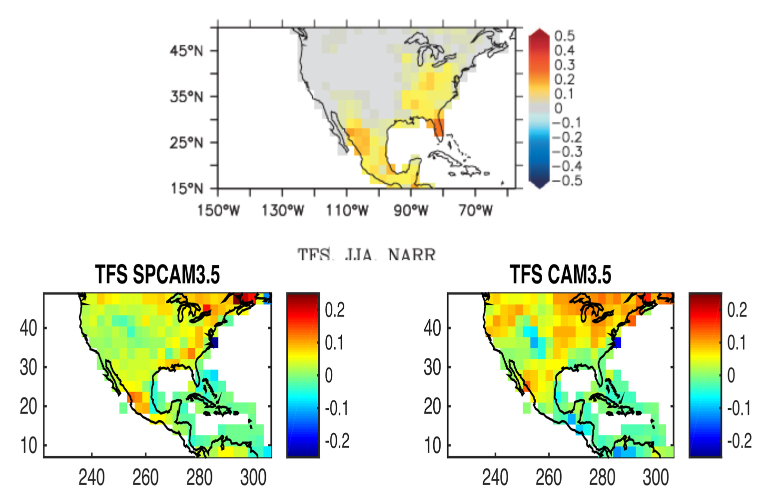


Figure 4: TFS of NARR (figure from Berg at al. 2013) and models in North America.

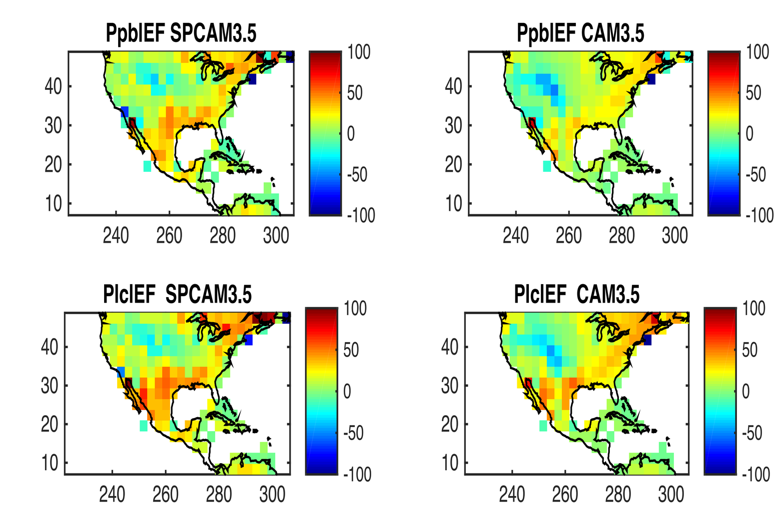


Figure 5: PBL height and LCL coupling strength with EF in North America.

$$\mathrm{normTFS} = \frac{\overline{\mathrm{EF}}}{\overline{\Gamma(r)}} \frac{\partial \Gamma(r)}{\partial \mathrm{EF}} = \frac{\overline{\mathrm{EF}}/\overline{\Gamma(r)}}{\sigma_{\mathrm{EF}}} \mathrm{TFS} \qquad \mathrm{normAFS} = \frac{\overline{\mathrm{EF}}}{\overline{\mathrm{E}[r]}} \frac{\partial \mathrm{E}[r]}{\partial \mathrm{EF}} = \frac{\overline{\mathrm{EF}}/\overline{\mathrm{E}[r]}}{\sigma_{\mathrm{EF}}} \mathrm{AFS}$$

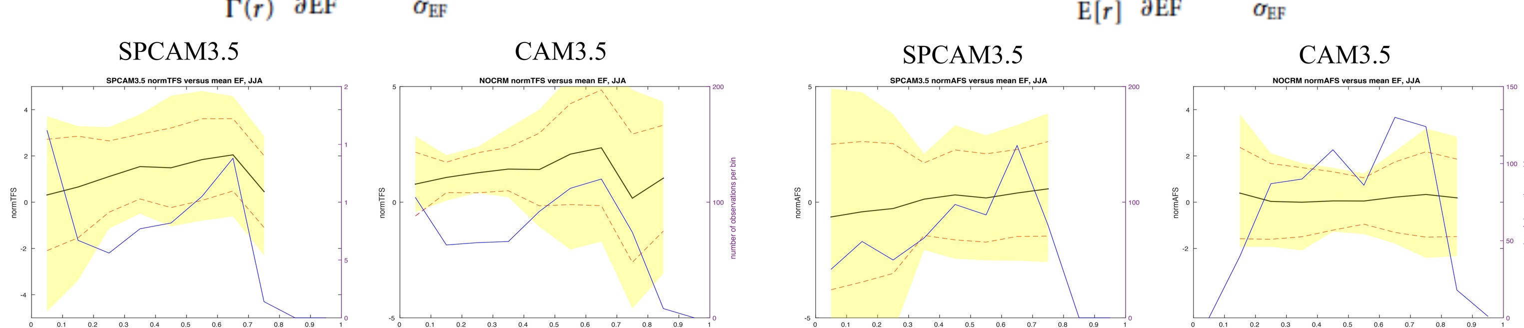


Figure 6: Function relationship of normalized TFS and AFS indices and EF of SPCAM3.5 and CAM3.5 in North America.

- Globally, TFS signal is weakened, and AFS signal is strengthened in SPCAM3.5 (Fig.3).
- In North America, SPCAM3.5 displays strong TFS signal along the east coast and Mexico that agrees with the results of NARR. In contrast, CAM3.5 has unobserved TFS hotspots in central and northwestern US instead of the east coast (Fig. 4)
- The spatial patterns of PBL height and LCL (lifting condensation level) variations with EF generally match the TFS signal in SPCAM3.5, but not in CAM3.5 (Fig. 5). That is, TFS model differences occur despite PBL property similarities
- Normalized TFS increases slightly with EF in both models, as observed. An observed insensitivity of normalized AFS to EF is more obvious in CAM3.5 (Fig. 6).

## LoCo - Mixing diagram

Taking advantage of the mixing diagram approach (Santanello et al. 2009) in order to better understand the mechanisms behind the model differences of land – atmosphere coupling signals.

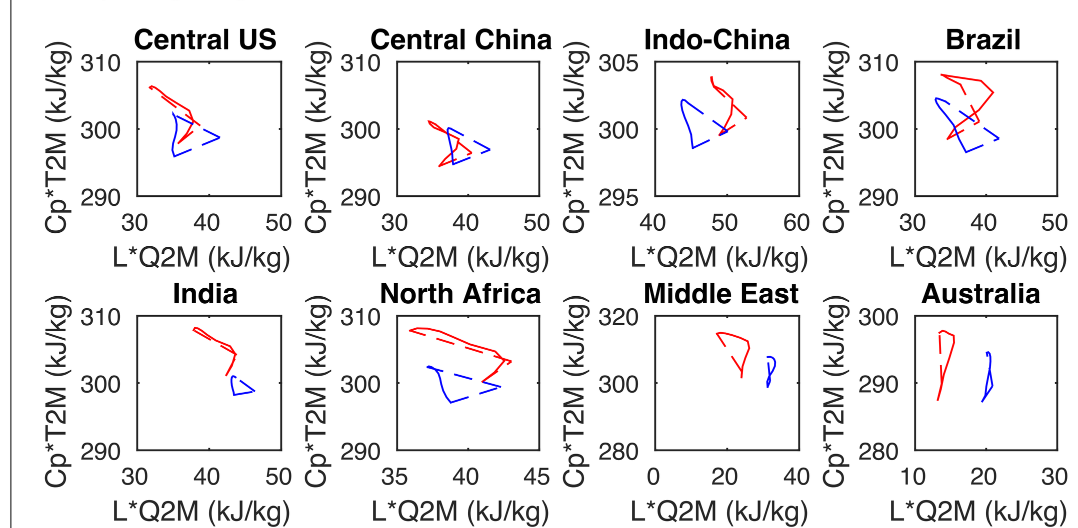


Figure 7. Mixing diagrams of SPCAM3.5 (red) and CAM3.5 (blue) with 2m temperature and humidity during daytime (LST 8am-5pm) in eight grids globally.

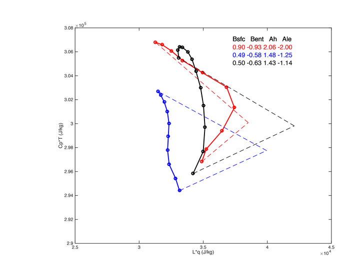


| | Hsfc (W/m^2) | Hent (W/m^2) | Htot (W/m^2) | LEsfc (W/m^2) | LEent (W/m^2) | LEtot (W/m^2) |
|---|---|---|---|---|---|---|
| OBS | 109 | 157 | 266 | 217 | -248 | -31 |
| SPCAM | 130 | 268 | 398 | 145 | -289 | -144 |
| CAM | 98 | 145 | 243 | 199 | -248 | -49 |

Figure 8. Mixing diagrams and the PBL energy budget at the Southern Great Plains (SGP) in America.

- The 2m trajectory of temperature and humidity has a bigger curvature in SPCAM3.5, associated with surface moistening in the early morning then drying during the rest of day. CAM3.5 has weaker diurnal surface moisture cycle at most locations (Fig. 7).
- Comparing with observations (ARMBE) at SGP, the results indicate the moistening process during early morning in SPCAM3.5 is reasonable, but the humidity amplitude of the diurnal variation is unreasonable large (Fig. 8).
- SPCAM3.5 has more heating and drying fluxes in the PBL, associated with deeper and faster PBL growth (not shown). Even though the bulk daytime mean fluxes are close (between CAM3.5 and ARMBE), the diurnal processes could be very different.

**Take-home points**:

- According to Dirmeyer et al. indices, explicit convection alters the geographic distribution of strong terrestrial segment coupling regions although the overall magnitude does not change much globally.
- According to Findell et al. indices, explicit convection lessens TFS signal (rainfall triggering), while slightly strengthening the AFS signal (rainfall amount).
- Mixing diagrams show superparameterized model with explicit convection contains an early morning moistening process that is not captured by conventional CAM.

References:
Berg, A., Findell, K., Lintner, B.R., et al., (2013). Precipitation sensitivity to surface heat fluxes over North America in reanalysis and model data. Journal of Hydrometeorology, 14(3).
Dirmeyer, P.A., (2011). The terrestrial segment of soil moisture-climate coupling. Geophysical Research Letters, 38.
Findell, K.L., Gentine, P., Lintner, B.R., and Kerr, C., (2011). Probability of afternoon precipitation in eastern United States and Mexico enhanced. Nature Geoscience, 4, 434-439.
Santanello, J.A., Peters-Lidard, C.D., Kumar, S.V., ea al., (2009). A modeling and observational framework for diagnosing local land-atmosphere coupling on diurnal time scales, Journal of Hydrometeorology, 10, 577-599.

Acknowledgements:
Jian Sun and Mike Pritchard were supported by funding from the DOE Early Career Program through DE-SC0012152.
Thanks to Marat Khairoutdinov, Dave Randall & CMMAP for developing & distributing SPCAM3.5.
Thanks to the NSF Extreme Science and Engineering Environment (XSEDE) for computing time